Liver iron content measurement using quantitative susceptibility mapping

Alexey Dimov[1,2], Pascal Spincemaille[3], Carlo Salustri[3], Tian Liu[4], Bo Xu[1,2], and Yi Wang[1,2]

[1]*Biomedical Engineering, Cornell University, Ithaca, NY, United States,* [2]*Radiology, Weill Cornell Medical College, New York, NY, United States,* [3]*Radiology, Weill Cornell Medical College, NY, United States,* [4]*MedimageMetric LLC, NY, United States*

TARGET AUDIENCE: Researchers interested in quantification of fat, iron and magnetic susceptibility (QSM) in the liver.

PURPOSE: The liver is known to allow various degrees of iron (hemochromatosis) and triglyceride (steatosis) accumulation within its cells, which strongly affect the MRI signal. Iron deposition is normally evaluated via R2* mapping [1]. However, R2* provides only an indirect measure of the iron stores which is affected by local tissue oxygenation, local vessel distribution and field inhomogeneity such as those near the lung-liver interface. These confounders also affect the necessary separation of fat and water signals and consequently the estimation of the fat fraction, which is relevant for liver disease treatment. By capitalizing on the difference between iron and fat susceptibilities, quantitative susceptibility mapping (QSM) may be used for the characterization of liver composition [2]. However, QSM requires an estimation of the total susceptibility field as an input and several confounding factors must be taken into account when applying this technique to abdominal studies: i) sharp air-tissue susceptibility interfaces (~9 ppm) and signal voids, ii) the presence of fat, which makes field estimation a nonlinear problem, iii) scan time constraints due to the necessity of using breath holding. In this work, we propose to use a multi-echo flow compensated 3D spiral acquisition, combined with an adaptive determination of fat content and magnetic susceptibility to quantify iron content in healthy livers.

METHODS: 1) Data acquisition: With IRB approval and informed consent, 8 healthy volunteers were scanned on a 1.5T MRI system (GE Excite HD, Milwaukee, WI), using an 8-channel cardiac coil and a 4-echo flow-compensated spiral sequence (TE = 0.6ms, ΔTE= 6.6ms, 4 echoes, TR = 25 ms, FA=30°, BW=±62.50 kHz, 48 spiral leafs, breath hold ~45 seconds and voxel size = 1.4×1.4×3mm^3). As a comparison, the 2D multi-echo SPGR sequence that is currently used in our clinical practice for the estimation of R2* and iron content was performed as well. Imaging parameters were TE = 1.3ms, ΔTE= 1.5ms, 16 echoes, TR = 28 ms, FA = 20°, BW=±62.50 kHz, 5 slices). **2) Total susceptibility field estimation:** A linear fitting of the signal phase was performed as a first step. Discontinuities in the field map between neighboring voxels caused by chemical shift were detected by searching for field differences of approximately $n/\Delta TE + mf_1^{(0)}$, where $f_1^{(0)}$ is the assumed chemical shift, n is an integer and $m = 0$ or 1. Both of these steps were performed with a magnitude-guided field unwrapping algorithm. The background field of this processed field map was estimated using PDF and then served as the initial guess for the inhomogeneity field in the IDEAL algorithm. Water and fat maps were estimated using a single peak fat model: $s(TE_n) = e^{-i2\pi f_s TE_n}(\rho_0 + \rho_1 e^{-i2\pi f_1 TE_n})$, where f_s is the total susceptibility field and ρ_0 and ρ_1 the water and fat contributions to the complex signal of a voxel at TE = 0. In the next step, both water and fat were assumed to have constant chemical shifts and magnetic susceptibilities. With this assumption, a piece-wise constant inversion of the magnetic field distribution [3] was used to estimate the water and fat susceptibilities and fat chemical shift. The latter manifested itself as that part of the field inside the fat map that could not be explained by a susceptibility that was constant within the water map and within the fat map. All above steps were then repeated with an updated chemical shift $f_1^{(k)} = f_1^{(k-1)} + \Delta f_1^{(k)}$,where k is the iteration step and $\Delta f_1^{(k)}$ was the residual chemical shift obtained from the piece-wise constant susceptibility mapping method. This process was repeated until the chemical shift correction $\Delta f_1^{(k)}$ fell below a preset threshold of 1 Hz. The obtained field map $f_s^{(k)}$ was passed to MEDIN [4] for the calculation of the quantitative susceptibility map. An ROI was drawn on one slice of the resulting QSM by encompassing the liver and excluding all major hepatic vessels as much as possible. The mean susceptibility value of this liver ROI was then recorded. From the 2D multi-echo SPGR data, the R2* was computed and linearly correlated across volunteers against the liver susceptibility value from QSM.

RESULTS: Liver QSM results are illustrated in Fig.1: axial plane shows a middle liver slice with vena cava, aorta, and branches of the right and middle hepatic veins visible (Fig. 1a); a coronal plane shows branching of the right hepatic vein (Fig. 1b) and vena cava. QSM values in liver relative to that of subcutaneous fat (Fig.2a) and back muscle (Fig.2b) for all volunteers were found to be well correlated with R2* ($p<0.01$).

DISCUSSION AND CONCLUSIONS: The proposed algorithm successfully reconstructed a susceptibility map in the liver, while minimizing the number of streaking artifacts typical for incomplete solutions of QSM. Features of interest, such as hepatic veins and portal veins were well visualized, while liver susceptibility was found to correlate with liver R2*.

REFERENCES: [1] Wood JC. Magnetic Curr Opin Hematol 2007;14:183. [2] Hernando D et al, MRM 2013 (Epub) [3] de Rochefort, L et al, MRM 2008 60(4), 1003 [4] Liu, T., et al. Magnet Reson Med 69, 467-476 (2013).

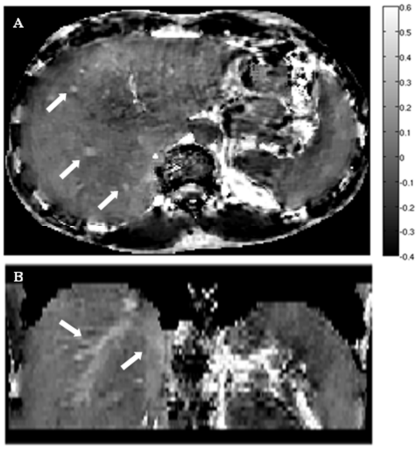

Fig.1 Axial (A) and coronal (B) slices of the reconstructed liver QSM. Note the contrast between hepatic parenchyma and hepatic veins

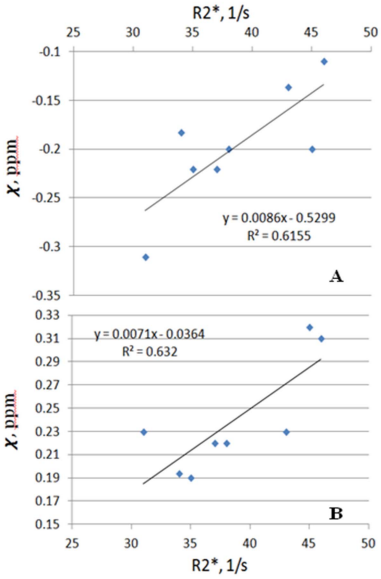

Fig.2 Comparison of correlations between liver R2* values and liver susceptibility relative to subcutaneous fat (A) and back muscle (B).